Neutral sphingomyelinase inhibition participates to the benefits of N-acetylcysteine treatment in post-myocardial infarction failing heart rats.

Christophe Adamy, Paul Mulder, Lara Khouzami, Nathalie Andrieu-Abadie, Nicole Defer, Gabriele Candiani, Catherine Pavoine, Philippe Caramelle, Richard Souktani, Philippe Le Corvoisier, et al.

Neutral sphingomyelinase inhibition participates to the benefits of N-acetylcysteine treatment in post- myocardial infarction failing heart rats

Christophe ADAMY[1,2,9], Paul MULDER[3,4,9], Lara KHOUZAMI[1,2], Nathalie ANDRIEU-ABADIE[5,6], Nicole DEFER[1,2], Gabriele CANDIANI[1,2], Catherine PAVOINE[1,2], Philippe CARAMELLE[1,2], Richard SOUKTANI[1,2], Philippe LE CORVOISIER[1,2,7,8], Magali PERIER[1,2], Matthias KIRSCH[2,8], Thibaud DAMY[1,2,8], Alain BERDEAUX[1,2,8], Thierry LEVADE[5,6], Christian THUILLEZ[3,4], Luc HITTINGER[1,2,8] and Françoise PECKER[1,2,8].

[1]Inserm, U841, Créteil, F- 94000, France; Université Paris12, IMRB, Faculté de Médecine, IFR10, Créteil, F- 94000 France; [3]Inserm, U644, Rouen, F-76183, France; [4]Université de Rouen, Faculté de Médecine et de Pharmacie, Rouen, F-76183, France; [5]Inserm, U858, Toulouse, F-31000, France; [6]Université Toulouse III Paul Sabatier, IFR31, Toulouse, F-31000, France; [7]Inserm, Centre d'Investigation Clinique 006, Créteil, F-94010, France; [8]AP-HP, Groupe hospitalier Henri Mondor-Albert Chenevier, Fédération de Cardiologie, Département de Chirurgie Cardiaque, Créteil, F-94010, France. [9]These authors contributed equally to this work.

Correspondence to Françoise Pecker, Inserm U841, Institut Mondor de Recherche Biomédicale, Hôpital Henri Mondor, 94000 Créteil, France. Phone: (33) 1 49 81 35 34; Fax: (33) 1 48 98 09 08; E-mail: francoise.pecker@creteil.inserm.fr

Running Head: NAC treatment in post-MI failing heart rat

Key words: chronic heart failure; glutathione; N-acetylcysteine; neutral sphingomyelinase; tumor necrosis factor-alpha.

ABSTRACT

Deficiency in cellular thiol tripeptide glutathione (L-γ glutamyl-cysteinyl-glycine) determines the severity of several chronic and inflammatory human diseases that may be relieved by oral treatment with the glutathione precursor N-acetylcysteine (NAC). Here, we showed that the left ventricle (LV) of human failing heart was depleted in total glutathione by 54%. Similarly, 2-month post-myocardial infarction (MI) rats, with established chronic heart failure (CHF), displayed deficiency in LV glutathione. One-month oral NAC treatment normalized LV glutathione, improved LV contractile function and lessened adverse LV remodelling in 3-month post-MI rats. Biochemical studies at two time-points of NAC treatment, 3 days and 1 month, showed that inhibition of the neutral sphingomyelinase (N-SMase), Bcl-2 depletion and caspase-3 activation, were key, early and lasting events associated with glutathione repletion. Attenuation of oxidative stress, downregulation of the pro-inflammatory cytokine tumor necrosis factor-α (TNF-α) and its TNF-R1 receptor were significant after 1-month NAC treatment. These data indicate that, besides glutathione deficiency, N-SMase activation is associated with post-MI CHF progression, and that blockade of N-SMase activation participates to post-infarction failing heart recovery achieved by NAC treatment. NAC treatment in post-MI rats is a way to disrupt the vicious sTNF-α/ TNF-R1/ N-SMase cycle.

1. INTRODUCTION

Oxidative stress and the proinflammatory cytokine tumor necrosis factor-α (TNF-α) are involved in the pathogenesis of several inflammatory and degenerative disorders [1-4], and are, in particular, major interrelated contributors to chronic heart failure (CHF) progression [5-9].

The tripeptide glutathione (L-γ glutamyl-cysteinyl-glycine) does not only play a key role in cell defence against oxidative stress, but also participates to many other metabolic cell functions [10]. We previously reported that glutathione status determines TNF-α adverse effects in heart [11, 12]. Herein we addressed the question as to whether glutathione deficiency might be causally linked to the exacerbated TNF-α activation occurring in well-established CHF, as this was observed in several other chronic diseases including HIV infection [13, 14], neurodegeneration [1, 15], muscular fatigue [14], rheumatoid arthritis [3] and chronic lung diseases [16, 17]. Of note, the well-being of the patients affected with those diseases is improved by treatment with the glutathione precursor N-acetylcysteine (NAC) [13, 14, 18, 19]. Previous studies pointed out the decrease in cardiac GSH/ GSSG ratio in CHF [20, 21]. However, the possible deficiency in total glutathione in the failing heart, and its related possible metabolic consequences have been overlooked.

TNF-α is not expressed in the normal heart but is upregulated in the failing heart [7, 22, 23]. TNF-α exerts its main biological functions in its soluble form (sTNF-α), binding to the membrane TNF-R1 receptor that mediates multiple distinct pathways [24], including oxidative stress and neutral sphingomyelinase (N-SMase) activation. Noteworthy, both pathways are subdued by glutathione. In its both reduced (GSH) and oxidized (GSSG) forms, glutathione serves as a natural inhibitor of N-SMase [25], which hydrolyzes sphingomyelin into ceramide, controlling the sphingolipid signaling cascade [26-28] and mediating TNF-α apoptotic [29] and negative inotropic effects in cardiomyocytes [11, 30, 31]. Downstream ceramide generation, the ordered cascade of events in N-SMase pathway comprises downregulation of the prosurvival factor Bcl-2, resulting into a decrease of the proapoptotic Bax/ prosurvival Bcl-2 protein ratio that in turn elicits activation of caspase-3 [32].

We have chosen the model of post-myocardial infarction (MI) rat, displaying a cardiac disease relevant with that of elderly and/or established CHF patients [33]. We show that total cardiac left ventricle (LV) glutathione is depleted in CHF patients and CHF post-MI rats. Glutathione repletion, achieved by oral NAC treatment in post-MI

rats, prompts cardiac function and tissue recovery. Inhibition of N-SMase/ Bcl-2/ caspase-3 pathway participates to the beneficial effects of NAC treatment.

2. MATERIALS AND METHODS

2.1. Patients

The usage of surgical heart samples unused for diagnostic purpose was in accordance with the legislation and good clinical practice in France. LV samples were collected from unused explanted hearts of patients undergoing transplantation for end-stage heart failure secondary to idiopathic dilated cardiomyopathy (n=3) or ischemic heart disease (n=3) (6 male, mean age of 52 ± 4 years, mean LV ejection fraction of 18 ± 4 %). Non -failing donor hearts (4 male and 2 female; mean age of 30 ± 3 years), which were unsuitable for transplantation for technical reasons, were used as controls. Myocardial tissue samples were obtained at the time of explant, immediately frozen in liquid nitrogen and stored at -80°C.

2.2. *Animals and experimental design*

Animal procedures were conducted in accordance with French government policies (Services Vétérinaires de la Santé et de la Production Animale, Ministère de l'Agriculture). The experimental design is described in **Fig.1**.

Induction of myocardial infarction (MI) in rats. We produced MI by ligation of the left coronary artery in 11 week-old male Wistar rats, anesthetized with Ketamine and Xylazine (60 and 5 mg/kg, respectively, intraperitoneally) [33]. MI resulted in a mean 41% infarct size (**Table 1**). Sham-operated rats were subjected to the same protocol, except that the snare was not tied.

NAC treatment. In the first series of experiment, after 2-month post-sham or post-MI operation, rats were randomized to receive no treatment (n=8 and 15 in sham-operated and post-MI groups, respectively), or NAC as food additive (120 $mg.kg^{-1}.day^{-1}$ for 1 month; n=11 and 15 in sham-operated and post-MI groups, respectively). Rats were euthanized at 3-months post-sham or post-MI operation. During the study period, 3 untreated MI rats and 2 NAC-treated MI rats died. Of note, 1-month NAC treatment had a small but significant positive effect on the cardiac function of sham rats (not shown).

Interpretation of the results obtained in 3-month post-sham and post-MI rats,

having received 1-month NAC treatment, did not allow separation of the early effects of NAC treatment from those related with the modifications of the patho-physiological status induced by long-term treatment. Thus, an additional series of experiments was performed, in which 2-month post-MI rats were euthanized after 3 days of NAC treatment. This 2-month study consisted of one single protocol, which included sham (n=6), untreated 2-month post-MI (n=11) and 3-day NAC-treated 2-month post-MI groups (n=11).

Echocardiographic and hemodynamics parameters of both 2- and 3-month sham groups were similar. Thus, for simplification, results were given in a unique sham group.

Echocardiography. Transthoracic Doppler echocardiographic studies, using an echocardiographic system (HDI 5000, ATL, USA) equipped with an 8.5 MHz probe, were performed in anesthetized rats (Brietal™; 50 $mg.kg^{-1}$, intraperitoneally) [33]. LV diameters were measured by the American Society of Echocardiology leading-edge method from at least 3 consecutive cardiac cycles [34]. LV outflow velocity was measured by pulsed-wave Doppler, and cardiac output was calculated as CO= aortic VTI x [π x (left ventricular outflow diameter/2)^2] x heart rate, where VTI is velocity-time integral.

LV hemodynamics. The right carotid artery was cannulated with a micromanometer-tipped catheter (SPR 407, Millar Instruments, USA) for recording arterial blood pressure, and the catheter was then advanced into the left ventricle for recording left ventricular pressures and its maximal and minimal rate of rise ($dP/dt_{max/min}$), and relaxation constant τ.

Animals were then euthanized, hearts were removed, rapidly frozen in isopentane cooled with liquid nitrogen, and stored at -80°C.

2.3. LV morpho-histological assessment

Heart sections were cut into 5 µm slices that were mounted onto slides (Superfrost Plus, Menzel-Glaser). Slices were stained with Sirius red F3BA (0.1% solution in saturated aqueous picric acid) to color collagen. Infarct size was calculated as (endocardial + epicardial circumference of the infarcted tissue)/(endocardial + epicardial circumference of the LV). as previously described [33]. Results obtained from 4 to 6 hearts were expressed as a percentage ± sem. Interstitial collagen density in the noninfarcted LV was quantified by examining 6-10 random high-power fields in each heart (magnification, x100). Images were analyzed using capture analyze Image-

Pro Plus 5.0 (Micromécanique). For each animal, one average value for interstitial fibrosis was calculated as percentage of collagen density. Results obtained from 5 to 6 hearts were expressed as a percentage ± sem. Mean cardiomyocyte cross-sectional area in the noninfarcted LV was determined in hematoxylin-eosin-stained slices by examining 4 random high-power fields in each heart (magnification, x200). Images were analyzed using a NIH Image analysis system. Results were obtained from 4 hearts in each group.

2.4. LV homogenate preparation and biochemical assays

The noninfarcted part of the LV was cut into 20 µm sections. Homogenates were prepared from 5 frozen sections of each LV by homogenization at 4°C, in 200 µl of 50 mM Hepes, pH 7.4, containing protease inhibitors (1mM PMSF, 2 µg/ ml leupeptin, 2 µg/ ml aprotinin), using disposable pestle/ microtube devices (Fisher Scientific Labosi).

Glutathione was measured in LV homogenates according to a modification of Tietze as previously described [12].

H_20_2 and lipid peroxidation by-products were quantified in LV homogenates using the Amplex Red Hydrogen Peroxide Kit (A22188) (Molecular Probes) and the Lipid peroxidation kit (Calbiochem), respectively.

N-SMase activity was determined in LV homogenates as previously described [11].

sTNF-α and TNF-R1 were quantified in LV homogenate fractions, obtained after centrifugation at 4°C at 20,000xg for 20 min. The supernatant, containing sTNF-α, was stored at –80°C until use. The pellet, containing the membrane fraction, was resuspended by homogenization in the Hepes buffer containing protease inhibitors, and 1% Triton X-100. After 30 min incubation on ice, the suspension was centrifuged at 20,000 x g for 20 min to remove debris, and the supernatant, containing the solubilized membrane-bound TNF-R1, was stored at -80°C until use. sTNF-α and TNF-R1 were quantified with ELISA kits (Quantikine, R&D Systems).

2.5. Western blot analysis

For Western blot analysis, proteins of the LV homogenate (caspase-3) or the 20,000 x g pellet fraction (Bcl-2 and Bax proteins) were resolved with 12.5% SDS-polyacrylamide gels using a 4% stacking gel. Proteins were transferred to polyvinylidene difluoride (PVDF) membranes (0.22 µm, Millipore) by electroblotting.

Membranes were next incubated with primary antibodies (anti-Bax, 1:1000 dilution, Cell Signaling; anti-Bcl-2, 1:850 dilution, R&D; anti-caspase-3, 1:1000 dilution, Cell Signaling) then with peroxydase-conjugated donkey anti-mouse or anti-rabbit IgG as appropriate (1:10,000 dilution, Jackson Immunoresearch). Immunodetected proteins were visualized by using the ECL Plus Western blotting detection system (Amersham) and quantified by scanning densitometry using a NIH Image anlysis system. Loading and protein transfers were verified with a mouse anti-ß-actin antibody (1:5,000, Sigma).

2.6. RNA preparation and RT-PCR

Total RNA were extracted from 5 pooled frozen LV sections, using Tri reagent (Sigma). Semi-quantitative RT-PCR was carried out on a Light Cycler (Roche Diagnostic), as previously described [35]. Oligonucleotide primers (MWG Biotech) were as follows: Rat *18S*, 5'-GTAACCCGTTGAACCCCATT-3' (sense) and 5'-CCATCCAATCGGTAGTAGCG–3' (antisense); rat *ANP*, 5'-AGCGAGCAGACCGATGAAGC-3' (sense) and 5'-GCAGAGTGGGAGAGGTAAGGC-3' (antisense); rat *ßMHC*, 5'-ATTCTCCTGCTGTTTCTTTACTTG-3' (sense) and 5'-TGACTTTGCCACCCTCTCG-3' (antisense). The PCR-amplified products were controlled on a 2% agarose gel and sequenced.

2.7. Statistical analysis

Results are given as means ± sem of determinations done in at least 5 different LV. Because measurements of echocardiographic, hemodynamics and biochemical parameters gave similar results for the 2- and 3-month sham subgroups, for simplification, data were pooled into one sham group. Data were analyzed by the Mann-Whitney test (GraphPad Software Inc). Differences were considered statistically significant at $P < 0.05$.

3. RESULTS

3.1. Deficiency in glutathione is a common feature of failing human LV and failing post-MI rat LV.

We analyzed total glutathione content in LV samples of unused explanted hearts from normal individuals and from patients with end-stage dilated or ischemic cardiomyopathies. Total glutathione content was decreased by 54% in failing human LV compared with control (**Fig. 2a**). Total glutathione was also decreased by 40% in the 2- and 3-month post-MI rats (**Fig.2b**).

Next, we examined whether glutathione repletion achieved by oral treatment with NAC might improve heart recovery in post-MI rats.

3.2. In post-MI rats, 1-month NAC treatment replenished LV glutathione, improved LV function and reduced LV fibrosis.

Transthoracic echocardiography showed marked deterioration in LV contractile function of 2-month post-MI rats compared to sham rats, as expressed by reduced percent fractional shortening (FS; **Table 1**). Systolic and diastolic functions were also markedly lessened, as illustrated by marked decrease in cardiac output and LV dP/dtmax, and increase in Tau relaxation factor and LV dP/dtmin, respectively (**Table 1**). LV dysfunction did not significantly worsen in 3-month post-MI rats proving that 2-month post-MI rats displayed well-established CHF (**Table 1**).

One-month NAC treatment, given as food additive (120 $mg.kg^{-1}.day^{-1}$) to CHF 2-month post-MI rats, normalized LV glutathione (**Fig.2b**), and improved LV function in 3-month post-MI group compared to untreated 3-month post-MI rats, as demonstrated by significant recovery of FS, systolic and diastolic function (**Table 1**). NAC-treated 3-month post-MI rats also displayed a trend towards retrieval compared to 2-month post-MI rats that reached significance for cardiac output (**Table 1**). One-month NAC treatment had no effect on the systolic blood pressure of post-MI rats (**Table 1**). This finding is consistent with our previous report that NAC treatment improved the cardiac function in the L-NAME hypertensive rat model (rats treated with the nitric oxide synthase inhibitor, L-NAME), without lessening hypertension [12]. Nevertheless, the absence of change in blood pressure together with an increase in cardiac output, implies that NAC treatment decreases systemic vascular resistance.

LV dilatation and hypertrophy, as assessed by enlarged LV diameter (**Table 1**) and increased heart weight (HW), normalized to body weight (BW), are two features of post-MI hearts (**Fig.3a**). The increase in HW/ BW ratio in post-MI rats was consistent with the presence of enlarged cardiomyocytes (cross-sectional width 32.1±0.8µm to compare with sham: 23.5 ± 0.6 µm; $P<0.05$, **Fig.3b**), next to interstitial collagen deposits in the noninfarcted LV. Fibrosis (**Fig.3c**) and re-expression of fetal atrial

natriuretic peptide (ANP) and myosin heavy chain (MHC)-ß isoform genes (**Fig.3d**) attested to pathological hypertrophy [36-39]. One-month NAC treatment did not lessen hypertrophy (**Fig.3a**). In fact, large cardiomyocytes were apparent in noninfarcted LV of NAC-treated 3-month post-MI rats, close to collagen fibres (cross-sectional width: 27.7 ± 0.6 µm; *P*<0.05 *vs* sham) **(Fig.3b**). But, importantly, noninfarcted LV in NAC-treated 3-month post-MI rats displayed reduced fibrosis (**Fig.3c**) and decreased expression of ANP and MHC-ß genes expression (**Fig.3d**), which was consistent with the observed recovery of LV function in NAC-treated post-MI rats.

3.3. Glutathione repletion is associated with early and persisting Inhibition of N-SMase/ Bcl-2/ caspase-3 cascade, and with late reduction in sTNF-α expression and oxidative stress.

Next experiments aimed to get insight into the biochemical mechanisms underlying the functional and structural benefits of NAC treatment. The biochemical studies were performed at 3-day and 1-month time-points of NAC treatment given to 2 months post-MI rats. In fact, at the early 3-day time-point, NAC treatment had no effect on the cardiac phenotype of 2 months post-MI rats (**Table 1**), but partly replenished LV glutathione to 75% of its control level in sham rats (**Fig.2b**). Thus, examination of the biochemical parameters after 3-day NAC treatment should allow identification of the early mechanisms preceding and likely to drive changes in the cardiac patho-physiological status. Because N-SMase is a direct target of glutathione, and a sensitive sensor to changes in cellular glutathione [40], we focused on the N-SMase/ Bcl-2/ caspase-3 cascade. N-SMase was stimulated by about 2-fold in noninfarcted LV of post-MI rats, compared with sham LV (**Fig.4a).** In accordance with the scheme of N-SMase cascade pathway, and with previous observation that deficiency in glutathione leads to the degradation of Bcl-2 protein [41], Bcl-2 protein was decreased in the noninfarcted LV of 2- and 3-month post-MI rats, without significant alteration of Bax protein (**Fig.4b**, typical). The resulting 50-60% decrease in Bcl-2/Bax ratio (**Fig.4b**, densitometric evaluation) was associated with increased amount of cleaved caspase-3, 17/ 19 kDa fragments, illustrating caspase-3 activation (**Fig.4c**). One major finding of this study is that 3-day NAC treatment blunted N-SMase activation, replenished Bcl-2 content and inhibited caspase-3 activation in noninfarcted LV of 2-month post-MI rats (**Fig.4a-b-c**). Importantly, the reversal effect of NAC treatment on N-SMase activity, Bcl-2 expression and caspase-3 activity persisted after 1-month (**Fig.4a-b-c**).

sTNF-α, which is a major contributor to CHF progression, triggers N-SMase

activation through TNF-R1. As shown in **Fig. 5a**, and as previously reported [7], sTNF-α was not detectable in LV of sham rat (<10 pg sTNF-α/mg prot), but was markedly expressed in noninfarcted LV of 2- and 3-month post-MI groups (**Fig.5a**), whereas TNF-R1 protein expression was similar in sham and post-MI LV (**Fig.5b**). After 3-day NAC treatment, expression of sTNF-α and TNF-R1 remained unchanged in noninfarcted LV of 2-month post-MI rats. In contrast, 1-month NAC treatment reduced the expression of both proteins by 46% and 51%, respectively, in noninfarcted LV of 3-month post-MI rats (**Fig.5a-b**).

The decrease in oxidative stress injury brought by NAC treatment has been associated with regression of fibrosis in hypertensive rats with sub-acute LV remodelling [12] and in mice with hypertrophic cardiomyopathy [42]. In the noninfarcted LV of 2- and 3-month post-MI rats, H_2O_2 release, assessed as an index of reactive oxygen species production, and lipid peroxidation by-products (LPO) accumulation were increased by 5- to 7- and 2-fold, respectively, compared with sham rats (**Fig.6 a-b**). Three-day NAC treatment had no significant effect on the oxidative stress injury in noninfarcted LV of 2-month post-MI rats (**Fig.6 a-b**). But, as expected, after 1-month NAC treatment, H_2O_2 release and LPO resumed control values in LV of 3-month post-MI rats (**Fig.6 a-b**).

Taken together, these results suggesed that cardiac tissue and function recovery, brought by NAC treatment to the failing post-MI heart, were associated with decreased expression of sTNF-α and TNF-R1, inhibition of N-SMase and caspase-3, increase in Bcl-2/ Bax ratio and blunting of oxidative stress, illustrating the disruption of the vicious sTNF-α/ TNF-R1 signalling cycle.

4. DISCUSSION

The new findings of this study are twofold. Firstly, the failing human heart displays a deficiency in total glutathione that is reproduced in a rat model of post-MI failing heart. Secondly, replenishment in cardiac glutathione, achieved in post-MI rats by oral NAC treatment, elicits recovery of cardiac tissue and function.

Previous studies have pointed out changes in the redox status of glutathione in the failing heart [20], but have overlooked a possible deficiency in glutathione content. Likewise, trials with antioxidants in patients with risks of cardiovascular diseases included antioxidants such as vitamin-E and vitamin-C gave disappointing results [43], but ignored glutathione or glutathione precursors. Of note, antioxidants cannot indiscriminately be lumped together. Vitamin-E, vitamin-C and glutathione participate

in an antioxidant network in which glutathione plays a pivotal role, recycling other antioxidants and keeping them in their active state. Vitamins will not compensate for severe deficiency in glutathione synthesis. Furthermore, antioxidants also differ from each other because of unrelated antioxidant properties such as N-SMase inhibition by glutathione [25], sirtuin activation by resveratrol [44], inhibition of PMP22 expression by vitamin-C [45].

N-SMase activation is described as an early event in ischemia/ reperfusion injury [46, 47], that is persisting in the chronic failing heart of 2-and 3-month post-MI rats. Partial repletion in cardiac glutathione of 2-month post-MI rats after 3-day NAC treatment blunts N-SMase activation specifically, which is consistent with the previously reported N-SMase inhibitory effect of glutathione. In contrast, full repletion in cardiac glutathione of 3-month post-MI rats after 1-month NAC-treatment is not only associated with a persistent low N-SMase activity, but also with a decreased expression in sTNF-α/ TNF-R1. On its own, sTNF-α/ TNF-R1 triggers FAN-mediated N-SMase activation. Hence, one may expect that long-term normalization of N-SMase activity does not only rely on enzyme inhibition by glutathione, as after 3-day NAC-treatment, but also on the collapse of its activation by sTNF-α. In any way, an overall outcome of glutathione repletion is the disruption of the TNF-α/ TNF-R1/ N-SMase signalling cycle. In fact, the effects of NAC treatment resemble those provided by TNF-α or TNF-R1 ablation, opposite to the deleterious effects brought by sTNF-α overexpression [48]. Thus, ablation of TNF-R1 or TNF-α in mice leads to a better post-MI preservation of the cardiac function compared with post-MI WT mice [49, 50]. One-month post-MI LV of TNF-α ablated mice also displayed lower collagen volume than post-MI WT mouse LV [50]. Finally, in mice with TNF-α-induced CHF, TNF-R1 ablation preserves cardiac function [51].

Of note, caspase-3 activation in LV of 2- and 3-month post-MI rats was not associated with nuclear DNA fragmentation assessed by DAPI staining (not shown), a finding consistent with previous studies using different experimental models of heart failure, including that of post-ischemia/ reperfusion mouse overexpressing caspase-3 in the heart [52, 53]. In their study Condolleri et al. [52] showed that cardiac specific caspase-3 expression induced transient depression of cardiac function and abnormal nuclear and myofibrillar ultrastructural damage. And when subjected to myocardial ischemia-reperfusion, caspase-3 transgenic mice showed increased infarct size and a higher susceptibility to die. However, DNA laddering, used as the test for apoptosis, was similar in caspase-3 overexpressing mice and control mice, having undergone, or

not, ischemia/ reperfusion. Thus, this study provided evidence that partial activation of caspase-3 was compatible with life. Likewise, in isolated adult rat cardiomyocytes, Communal et al [54] have observed that, in the early phase of apoptosis when no major DNA cleavage occurred, caspase-3 activation elicited the cleavage of myofibrillar proteins. Hence, under conditions where the apoptotic response is not completed, caspase-3 activation is likely to damage nuclear and myofibrillar proteins, which will prompt contractile dysfunction before cell death.

Other mechanisms are prone to participate to the beneficial effects of NAC treatment. Thus, glutathiolation of caspase-3, relying on cellular glutathione availability, hinders TNF-α-induced, caspase-8-mediated enzyme cleavage [55]. Differently, the antioxidant capacity of NAC is considered as its major attribute. Indeed, 1-month NAC treatment reduced oxidative stress in post-MI hearts. However, in contrast to N-SMase activation, oxidative stress did not significantly lessen within 3-day NAC treatment. Hence, beneficial effects of NAC treatment to post-MI heart may rely on both non-antioxidant effects and the global antioxidant capacity of glutathione.

Finally, it should be noted that recovery of the contractile function promoted by NAC treatment is not only associated with the improvement of cardiac parameters, but also with a decrease in systemic vascular resistance. Because cardiac iNOS expression was increased in post-MI rats, and normalized after 1-month NAC treatment (not shown), the improvement of hemodynamic function in NAC-treated rats more likely relied on the blunting of oxidative stress, including the neutralization of reactive nitrogen species, rather than on a NO mediated vasodilatory effect [56, 57].

In cardiology, treatments with NAC were limited to acute syndromes [58]. Our results disclose NAC as a possible complementary treatment to current medical therapies for CHF patients.

ACKNOWLEDGMENTS

This work was supported by the Institut National de la Santé et de la Recherche Médicale, the Université Paris-Val-de Marne, the Association Française contre les Myopathies, the European Commission (IHP Network grant ”FLUOR MMPI” HPRN-CT-2002-00181) and the Agence Nationale de la Recherche.

We thank D. Charlemagne and D. Charue (Inserm U689), who provided left ventricular samples collected from unused explanted hearts of normal individuals, S. Lotersztajn for her helpful and constant guidance, J. Hanoune and G. Guellaën for helpful discussions and permanent support, F. Clerc for her skilful advice.

Table 1 : LV morphometric and functional parameters in sham and post-MI rats, untreated or given 3-day or 1-month NAC treatment started 2 months after MI.

	Sham rats[a]	2-month post-MI rats		3-month post-MI rats	
		Untreated	3-day NAC	Untreated	1-month NAC
	(*n*=14)	(*n*=11)	(*n*=11)	(*n*=12)	(*n*=13)
Organ morphometry					
Infarct size %	-	41 ± 3	41 ± 5	41 ± 8	46 ± 4
Echocardiography					
LV EDD (mm)	6.3 ± 0.1	9.8 ± 0.2#	10 ± 0.2#	9.5 ± 0.4#	9.4 ± 0.2#
LV ESD (mm)	3.2 ± 0.2	8.4 ± 0.2#	8.8 ± 0.2#	8.1 ± 0.4#	7.8 ± 0.2#
FS (%)	50 ± 2	15 ± 1#	15 ± 1#	13 ± 2#	17 ± 1#†
Cardiac output (ml/ min)	145 ± 3	110 ± 6#	107 ± 5#	101 ± 6#	124 ± 4#†‡
Hemodynamics					
SBP (mm Hg)	133 ± 5	113 ± 6#	118 ± 3#	107 ± 3#	111 ± 6#
Systolic function					
LV ESP (mm Hg)	124 ± 6	109 ± 7#	109 ± 6#	96 ± 5#	106 ± 7#
LV dP/dt_{max} (mm Hg/ s)	8790 ± 580	5940 ± 480#	6210 ± 380#	5360 ± 420#	7050 ± 540#†
Diastolic function					
LV EDP (mm Hg)	4 ± 1	11± 2#	15 ± 3#	16 ± 4#	6 ± 1#†
LV dP/dt_{min} (mm Hg/ s)	-8240 ± 580	-4790 ± 500#	-4720 ± 410#	-4000 ± 320#	-5220 ± 430#†
Tau (ms)	5 ± 0	16 ± 3#	16 ± 2#	16 ± 2#	11 ± 1#†

LV indicates left ventricle; **LV EDD**, LV end-diastolic diameter; **LV ESD**, LV end-systolic diameter; **FS**, LV fractional shortening defined as (LV EDD - LV end-systolic diameter/LV EDDx100; **SBP**, systolic blood pressure**; LVEDP**, LV end-diastolic pressure; **LVESP**, LV end-systolic pressure; **LV dP/dtmax**, LV pressure maximal rate of rise; **LV dP/dtmin**, LV pressure minimal rate of rise. [a]Because echocardiographic and hemodynamics parameters of 2- and 3-month sham groups were similar, for simplification, results were given in a unique sham group. #P<0.05 vs sham-operated group; †P<0.05 vs 3 month untreated MI group; ‡P<0.05 vs 2 month untreated MI group.

REFERENCES

[1] Allan SM, Rothwell NJ. Cytokines and acute neurodegeneration. Nat Rev Neurosci 2001; 2: 734-44.

[2] Aggarwal BB. Signalling pathways of the TNF superfamily: a double-edged sword. Nat Rev Immunol 2003; 3: 745-756.

[3] Feldmann M, Maini RN. TNF defined as a therapeutic target for rheumatoid arthritis and other autoimmune diseases. Nat Med 2003; 9: 1245-50.

[4] Joosten LA, et al. IL-32, a proinflammatory cytokine in rheumatoid arthritis. Proc Natl Acad Sci U S A 2006; 103: 3298-303.

[5] Mallat Z, et al. Elevated levels of 8-iso-prostaglandin F2alpha in pericardial fluid of patients with heart failure: a potential role for in vivo oxidant stress in ventricular dilatation and progression to heart failure. Circulation 1998; 97: 1536-9.

[6] Giordano FJ. Oxygen, oxidative stress, hypoxia, and heart failure. J Clin Invest 2005; 115: 500-8.

[7] Mann DL. Inflammatory mediators and the failing heart. Past, present, and the foreseeable future. Circ Res 2002; 91: 988-998.

[8] Springer J, von Haehling S, Anker SD. The need for a standardized definition for cachexia in chronic illness. Nat Clin Pract Endocrinol Metab 2006; 2: 416-7.

[9] Kaur K, Sharma AK, Dhingra S, Singal PK. Interplay of TNF-alpha and IL-10 in regulating oxidative stress in isolated adult cardiac myocytes. J Mol Cell Cardiol 2006; 41: 1023-30.

[10] Fratelli M, et al. Gene expression profiling reveals a signaling role of glutathione in redox regulation. Proc Natl Acad Sci U S A 2005; 102: 13998-4003.

[11] Cailleret M, et al. N-acetylcysteine prevents the deleterious effect of tumor necrosis factor-(alpha) on calcium transients and contraction in adult rat cardiomyocytes. Circulation 2004; 109: 406-11.

[12] Bourraindeloup M, et al. N-acetylcysteine treatment normalizes serum tumor necrosis factor-alpha level and hinders the progression of cardiac injury in hypertensive rats. Circulation 2004; 110: 2003-9.

[13] Herzenberg LA, et al. Glutathione deficiency is associated with impaired survival in HIV disease. Proc Natl Acad Sci U S A 1997; 94: 1967-1972.

[14] Droge W, Holm E. Role of cysteine and glutathione in HIV infection and other diseases associated with muscle wasting and immunological dysfunction. Faseb J 1997; 11: 1077-89.

[15] Andersen JK. Oxidative stress in neurodegeneration: cause or consequence? Nat Med 2004; 10 Suppl: S18-25.

[16] Moodie FM, et al. Oxidative stress and cigarette smoke alter chromatin remodeling but differentially regulate NF-kappaB activation and proinflammatory cytokine release in alveolar epithelial cells. Faseb J 2004; 18: 1897-9.

[17] Tirouvanziam R, et al. High-dose oral N-acetylcysteine, a glutathione prodrug, modulates inflammation in cystic fibrosis. Proc Natl Acad Sci U S A 2006; 103: 4628-33.

[18] Demedts M, et al. High-Dose Acetylcysteine in Idiopathic Pulmonary Fibrosis. N Engl J Med 2005; 353: 2229-2242.

[19] Hauer K, et al. Improvement in muscular performance and decrease in tumor necrosis factor level in old age after antioxidant treatment. J Mol Med 2003; 81: 118-125.

[20] Hill MF, Singal PK. Right and left myocardial antioxidant responses during heart failure subsequent to myocardial infarction. Circulation 1997; 96: 2414-20.

[21] Rozanski GJ, Xu Z. Glutathione and K(+) channel remodeling in postinfarction rat heart. Am J Physiol Heart Circ Physiol 2002; 282: H2346-55.

[22] Nian M, Lee P, Khaper N, Liu P. Inflammatory cytokines and postmyocardial infarction remodeling. Circ Res 2004; 94: 1543-53.

[23] Von Haehling S, Jankowska EA, Anker SD. Tumour necrosis factor-alpha and the failing heartPathophysiology and therapeutic implications. Basic Res Cardiol 2004; 99: 18-28.

[24] MacEwan DJ. TNF receptor subtype signalling: differences and cellular consequences. Cell Signal 2002; 14: 477-492.

[25] Liu B, Hannun YA. Inhibition of the neutral magnesium-dependent sphingomyelinase by glutathione. J Biol Chem 1997; 272: 16281-7.

[26] Adam-Klages S, et al. FAN, a novel WD-repeat protein, couples the p55 TNF-receptor to neutral sphingomyelinase. Cell 1996; 86: 937-47.

[27] Segui B, et al. Involvement of FAN in TNF-induced apoptosis. J Clin Invest 2001; 108: 143-51.

[28] Malagarie-Cazenave S, et al. Role of FAN in tumor necrosis factor-alpha and lipopolysaccharide-induced interleukin-6 secretion and lethality in D-galactosamine-sensitized mice. J Biol Chem 2004; 279: 18648-55.

[29] Krown KA, et al. Tumor necrosis factor alpha-induced apoptosis in cardiac myocytes. Involvement of the sphingolipid signaling cascade in cardiac cell death. J Clin Invest 1996; 98: 2854-65.

[30] Oral H, Dorn GW, 2nd, Mann DL. Sphingosine mediates the immediate negative inotropic effects of tumor necrosis factor-alpha in the adult mammalian cardiac myocyte. J Biol Chem 1997; 272: 4836-42.

[31] Amadou A, Nawrocki A, Best-Belpomme M, Pavoine C, Pecker F. Arachidonic acid mediates dual effect of TNF-alpha on Ca(2+) transients and contraction of adult rat cardiomyocytes. Am J Physiol Cell Physiol 2002; 282: C1339-47.

[32] Sawada M, et al. Ordering of ceramide formation, caspase activation, and Bax/Bcl-2 expression during etoposide-induced apoptosis in C6 glioma cells. Cell Death Differ 2000; 7: 761-72.

[33] Mulder P, et al. Long-term survival and hemodynamics after endothelin-a receptor antagonism and angiotensin-converting enzyme inhibition in rats with chronic heart failure: monotherapy versus combination therapy. Circulation 2002; 106: 1159-64.

[34] Sahn DJ, DeMaria A, Kisslo J, Weyman A. Recommendations regarding quantitation in M-mode echocardiography: results of a survey of echocardiographic measurements. Circulation 1978; 58: 1072-83.

[35] Pavoine C, et al. beta2-Adrenergic signaling in human heart: shift from the cyclic AMP to the arachidonic acid pathway. Mol Pharmacol 2003; 64: 1117-25.

[36] Chien KR, Knowlton KU, Zhu H, Chien S. Regulation of cardiac gene expression during myocardial growth and hypertrophy: molecular studies of an adaptive physiologic response. Faseb J 1991; 5: 3037-46.

[37] Milano CA, et al. Myocardial expression of a constitutively active alpha 1B-adrenergic receptor in transgenic mice induces cardiac hypertrophy. Proc Natl Acad Sci U S A 1994; 91: 10109-13.

[38] McConnell BK, et al. Comparison of two murine models of familial hypertrophic cardiomyopathy. Circ Res 2001; 88: 383-9.

[39] Perrino C, et al. Intermittent pressure overload triggers hypertrophy-independent cardiac dysfunction and vascular rarefaction. J Clin Invest 2006; 116: 1547-60.

[40] Liu B, et al. Glutathione regulation of neutral sphingomyelinase in tumor necrosis factor-alpha-induced cell death. J Biol Chem 1998; 273: 11313-20.

[41] Celli A, Que FG, Gores GJ, LaRusso NF. Glutathione depletion is associated with decreased Bcl-2 expression and increased apoptosis in cholangiocytes. Am J Physiol 1998; 275: G749-57.

[42] Marian AJ. Pathogenesis of diverse clinical and pathological phenotypes in hypertrophic cardiomyopathy. Lancet 2000; 355: 58-60.

[43] Jialal I, Devaraj S. Antioxidants and atherosclerosis: don't throw out the baby with the bath water. Circulation 2003; 107: 926-8.

[44] Parker JA, et al. Resveratrol rescues mutant polyglutamine cytotoxicity in nematode and mammalian neurons. Nat Genet 2005; 37: 349-50.

[45] Passage E, et al. Ascorbic acid treatment corrects the phenotype of a mouse model of Charcot-Marie-Tooth disease. Nat Med 2004; 10: 396-401.

[46] Hernandez OM, Discher DJ, Bishopric NH, Webster KA. Rapid activation of neutral sphingomyelinase by hypoxia-reoxygenation of cardiac myocytes. Circ Res 2000; 86: 198-204.

[47] O'Brien NW, et al. Factor associated with neutral sphingomyelinase activation and its role in cardiac cell death. Circ Res 2003; 92: 589-91.

[48] Diwan A, et al. Targeted overexpression of noncleavable and secreted forms of tumor necrosis factor provokes disparate cardiac phenotypes. Circulation 2004; 109: 262-8.

[49] Ramani R, et al. Inhibition of tumor necrosis factor receptor-1-mediated pathways has beneficial effects in a murine model of postischemic remodeling. Am J Physiol Heart Circ Physiol 2004; 287: H1369-77.

[50] Sun M, et al. Excessive tumor necrosis factor activation after infarction contributes to susceptibility of myocardial rupture and left ventricular dysfunction. Circulation 2004; 110: 3221-8.

[51] Higuchi Y, et al. Involvement of Reactive Oxygen Species-mediated NF- kappa B Activation in TNF- alpha -induced Cardiomyocyte Hypertrophy. J Mol Cell Cardiol 2002; 34: 233-40.

[52] Condorelli G, et al. Heart-targeted overexpression of caspase3 in mice increases infarct size and depresses cardiac function. Proc Natl Acad Sci U S A 2001; 98: 9977-82.

[53] Moorjani N, et al. Activation of apoptotic caspase cascade during the transition to pressure overload-induced heart failure. J Am Coll Cardiol 2006; 48: 1451-8.

[54] Communal C, et al. Functional consequences of caspase activation in cardiac myocytes. Proc Natl Acad Sci U S A 2002; 99: 6252-6.

[55] Pan S, Berk BC. Glutathiolation regulates tumor necrosis factor-alpha-induced caspase-3 cleavage and apoptosis: key role for glutaredoxin in the death pathway. Circ Res 2007; 100: 213-9.

[56] Levrand S, et al. Peroxynitrite is a major trigger of cardiomyocyte apoptosis in vitro and in vivo. Free Radic Biol Med 2006; 41: 886-95.

[57] Lewis SJ, et al. Differential effects of peroxynitrite on the function of arginine vasopressin V(1a) receptors and alpha(1)-adrenoceptors in vivo. Vascul Pharmacol 2007; 46: 24-34.

[58] Sochman J. N-acetylcysteine in acute cardiology: 10 years later: what do we know and what would we like to know?! J Am Coll Cardiol 2002; 39: 1422-8.

LEGENDS TO FIGURES

Fig.1: Experimental procedure. The 5 groups of rats consisted of sham (n=14); untreated 2- and 3-month post-MI rats (n=11 and 15, respectively); treated 2-month post-MI rats having received NAC as food additive (120 $mg.kg^{-1}.day^{-1}$) during the 3 days preceding euthanasia (n=11); treated 3-month post-MI rats having received 1 month NAC treatment, initiated 2 months after ligation (n=15).

Fig.2: Deficiency in glutathione is a common feature of failing human and post-MI rat LV. (a) Total glutathione was measured in LV samples of unused explanted hearts from normal individuals (control, n=6) and from patients with end-stage with dilated or ischemic cardiomyopathies (failing, n=6). (b) Rat groups are as specified in the legend to Fig.1. Total glutathione was measured in noninfarcted LV samples from rats of the 5 groups. Mean ± s.e.m. from 11 to 14 left ventricle samples. #P<0.05 *vs* sham group; †P<0.05 for NAC-treated *vs* corresponding 2- or 3-month post-MI untreated groups.

Fig.3: Failing post-MI rat LV displays pathological remodeling as illustrated by hypertrophy, fibrosis, fetal gene re-expression. One-month NAC treatment reduces fibrosis and normalizes fetal gene expression. Rat groups are as specified in the legend to Fig.1. (a) Hypertrophy. Heart weight (HW) normalized to body weight (BW). Mean ± s.e.m. from 12 to 14 animals. (b) Hematoxylin-eosin-stained areas (original magnification, X 200; scale bars, 50µm) of sham LV cross-sections, and noninfarcted LV cross-sections from untreated and NAC-treated 3-month post-MI rats in fibrotic regions characterized by the presence of large cardiomyocytes. (c) Fibrosis. Quantitative morphometric analysis of interstitial fibrosis in LV sections from sham rats and noninfarcted LV sections from untreated and NAC-treated 3-month post-MI rats, and representative sirius red staining (original magnification, X100). Mean ± s.e.m. from 5 to 6 LV samples. (d) Fetal gene expression. Quantitative RT-PCR analysis of ANP and ßMHC gene expression in noninfarcted LV of untreated and NAC-treated 3-month post-MI rats, relative to mRNA expression in LV of sham rat. Mean ± s.e.m. from 6 noninfarcted LV samples. #P<0.05 *vs* sham group; †P<0.05 for NAC-treated *vs* untreated 3-month post-MI group.

Fig.4: Inhibition of N-SMase / Bcl-2 / caspase-3 pathway is an early and sustained event associated with glutathione repletion in NAC-treated post-MI rat

LV. Rat groups are as specified in the legend to Fig.1. (a) N-SMase activity was assayed in LV of sham rats and noninfarcted LV of untreated and NAC-treated 2- and 3-month post-MI rats. Mean ± s.e.m. from 8 to 12 LV samples for untreated and NAC-treated 2- and 3-month post-MI groups. (b) Representative Western blots analysis of Bcl-2 and Bax proteins in LV of sham rats and noninfarcted LV of 2- and 3-month post-MI untreated and NAC-treated, and densitometric evaluation expressed as Bcl-2/ Bax ratio. Mean ± s.e.m. from 8 to 12 LV samples. (c) Representative Western blots analysis of full length (35 kDa) and large fragments (17/ 19 kDa) of cleaved caspase-3 in LV of sham rats and noninfarcted LV of 2- and 3-month post-MI untreated and NAC-treated, and densitometric evaluation expressed as cleaved/ total ratio. Mean ± s.e.m. from 6 LV samples. #P<0.05 *vs* sham group; †P<0.05 for NAC-treated *vs* corresponding 2- or 3-month post-MI untreated groups.

Fig.5: One-month NAC treatment decreases sTNF-α and TNF-R1 expression in failing post-MI rat LV. Rat groups are as specified in the legend to Fig.1. (a) sTNF-α was quantified by ELISA in LV of sham rats and noninfarcted LV of untreated and NAC-treated 2- and 3-month post-MI rats. Mean ± s.e.m. from 8 to 12 LV samples. (b) TNF-R1 was assayed by ELISA in LV of sham rats and noninfarcted LV of untreated and NAC-treated 2- and 3-month post-MI rats. Mean ± s.e.m. from 8 to 12 LV samples. #P<0.05 *vs* sham group; †P<0.05 for NAC-treated *vs* untreated 3-month post-MI group.

Fig.6: One-month NAC treatment decreases oxidative stress injury in failing post-MI rat LV. Rat groups are as specified in the legend to Fig.1. Oxidative stress is assessed by (a) H_2O_2 release and (b) LPO accumulation in LV of sham rats 9and noninfarcted LV of untreated and NAC-treated, 2- and 3-month post-MI rats. Mean ± s.e.m. from 8 to 12 LV samples. #P<0.05 *vs* sham group; †P<0.05 for NAC-treated *vs* untreated 3-month post-MI group.

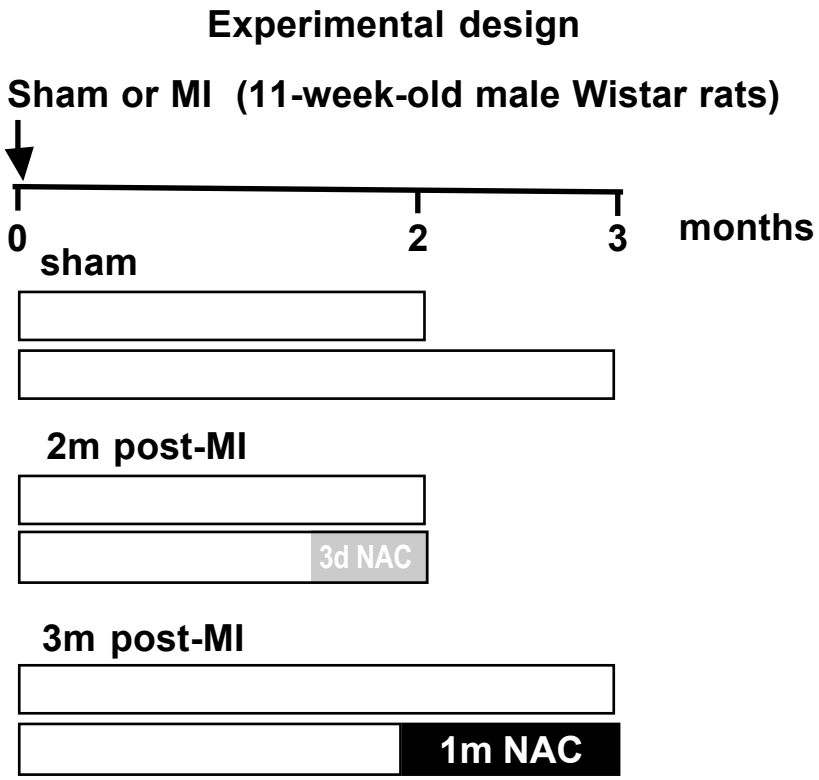

Figure 1

a

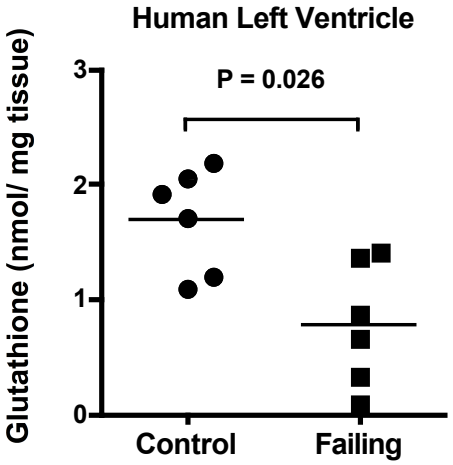

b

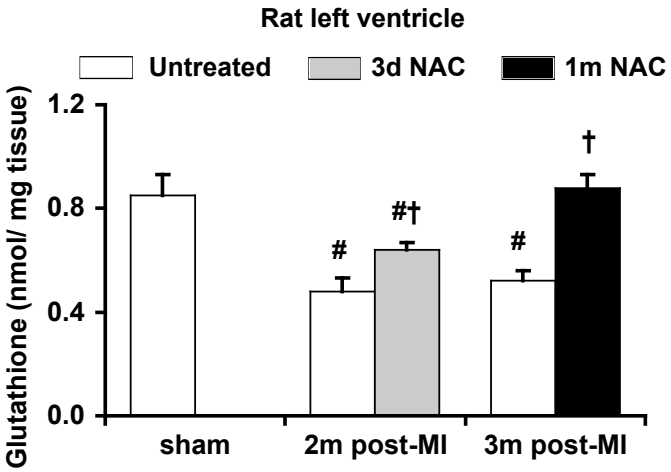

Figure 2

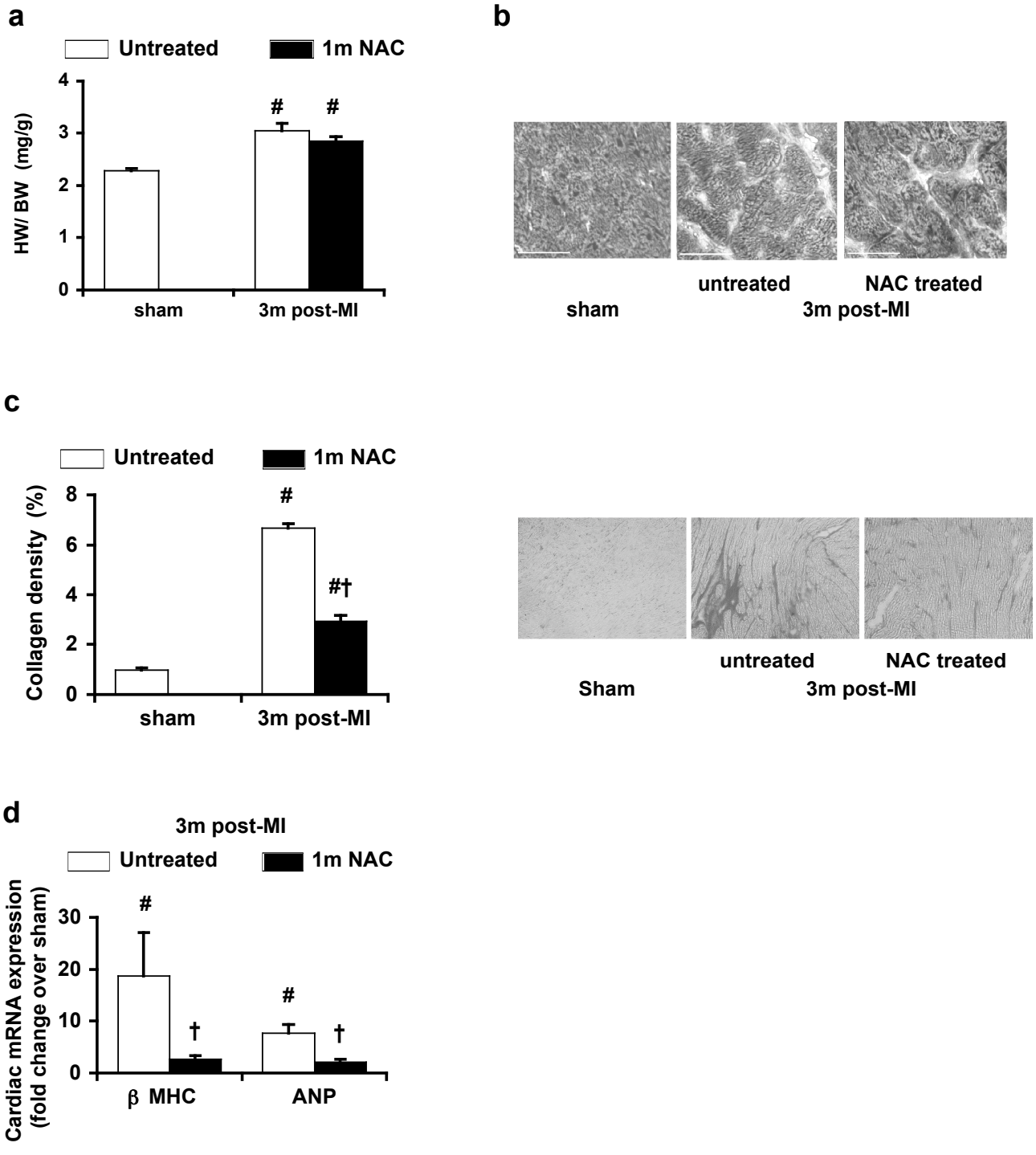

Figure 3

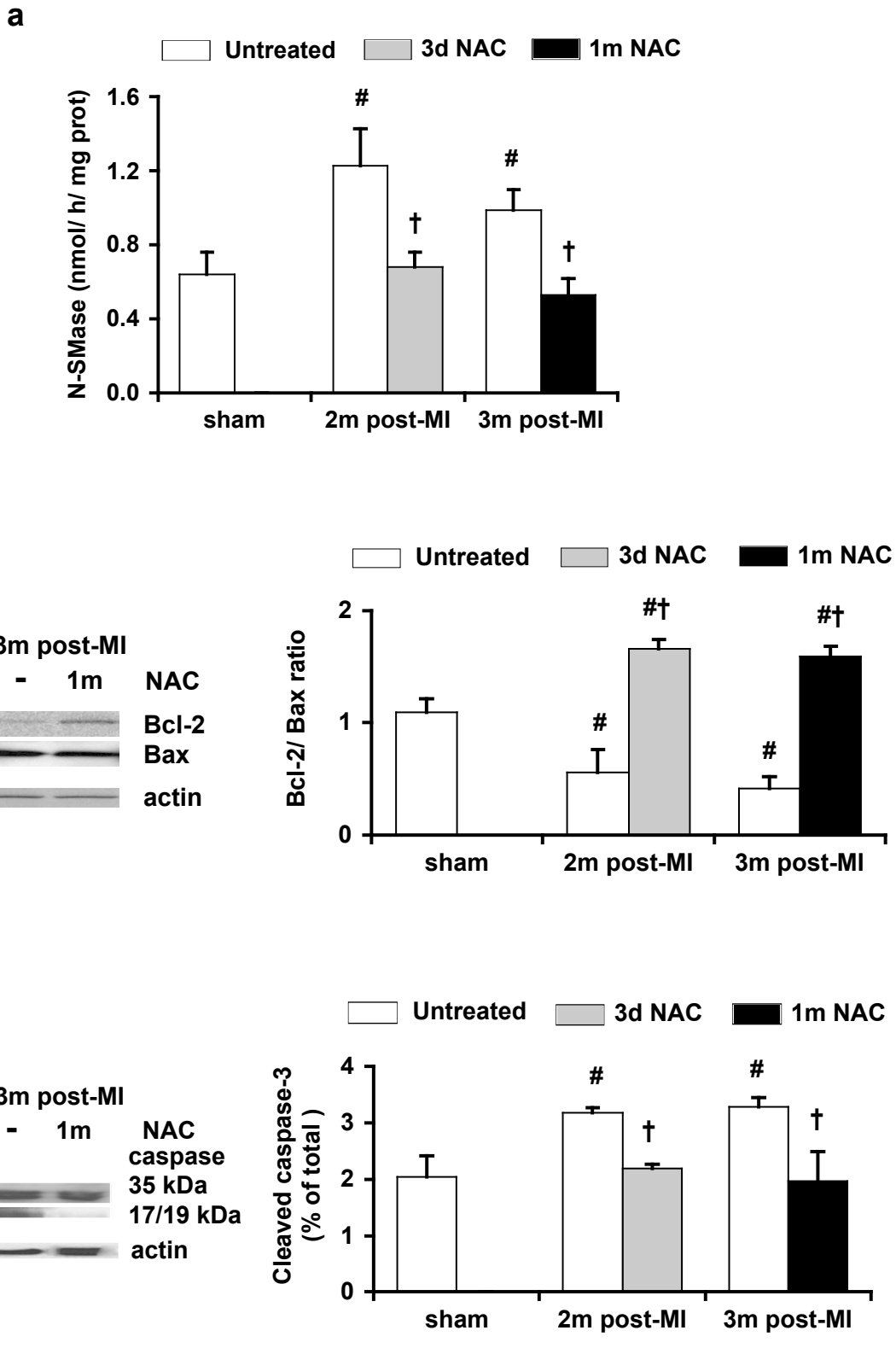

Figure 4

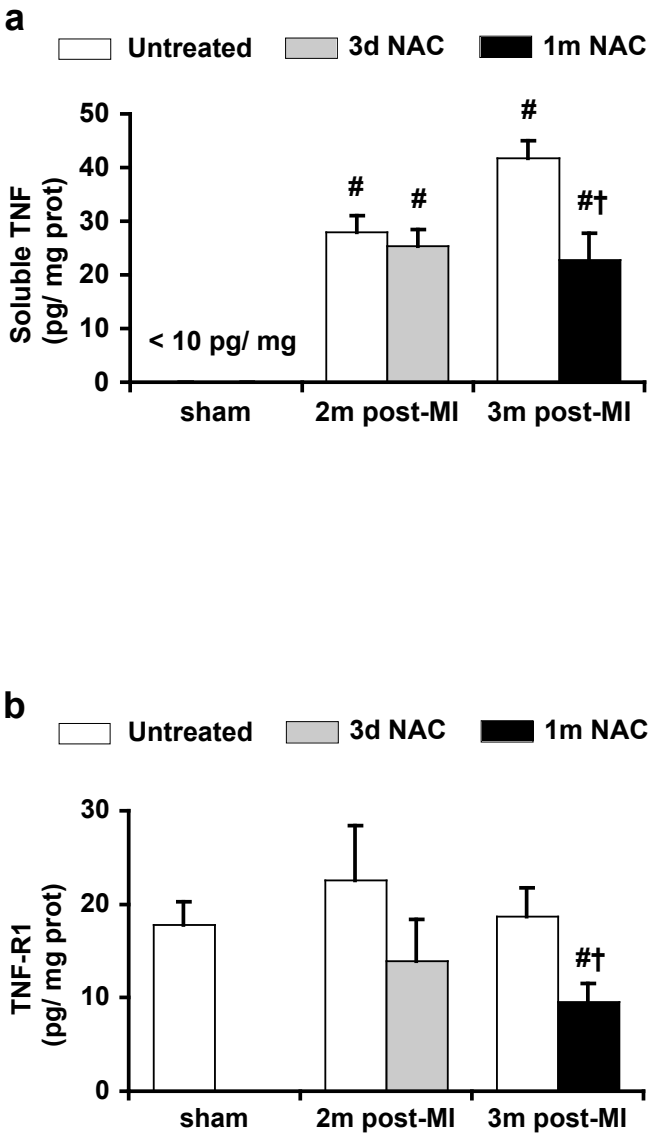

Figure 5

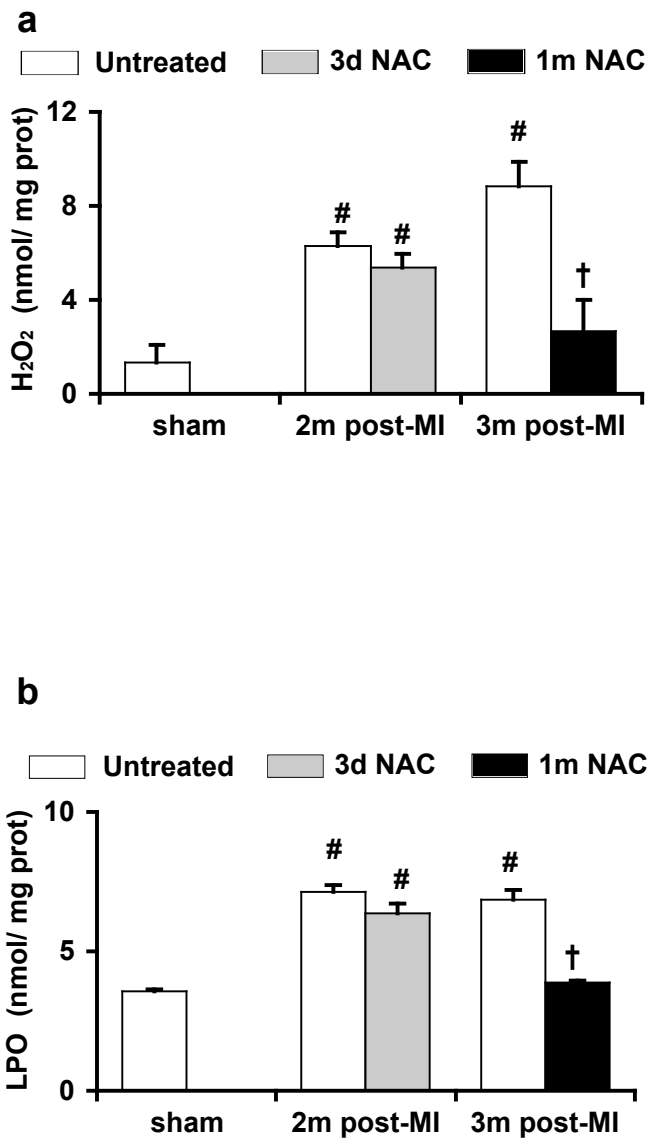

Figure 6